Biochimica et Biophysica Acta 1814 (2011) 1974–1983

Contents lists available at ScienceDirect

Biochimica et Biophysica Acta

journal homepage: www.elsevier.com/locate/bbapap

Catalytic oxidation of *o*-aminophenols and aromatic amines by mushroom tyrosinase

Jose Luis Muñoz-Muñoz [a], Francisco Garcia-Molina [a], Pedro Antonio Garcia-Ruiz [b], Ramon Varon [c], Jose Tudela [a], Jose N. Rodriguez-Lopez [a], Francisco Garcia-Canovas [a,*]

[a] *GENZ: Grupo de Investigación Enzimología, Departamento de Bioquímica y Biología Molecular-A, Facultad de Biología, Universidad de Murcia, E-30100, Espinardo, Murcia, Spain*
[b] *QCPAI: Grupo de Química de Carbohidratos, Polímeros y Aditivos Industriales, Departamento de Química Orgánica, Facultad de Química, Universidad de Murcia, E-30100, Espinardo, Murcia, Spain*
[c] *Departamento de Química-Física, Escuela de Ingenieros Industriales de Albacete, Universidad de Castilla la Mancha, Avda, España s/n, Campus Universitario, E-02071, Albacete, Spain*

ARTICLE INFO

Article history:
Received 11 May 2011
Received in revised form 12 July 2011
Accepted 13 July 2011
Available online 22 July 2011

Keywords:
Tyrosinase
Aromatic amine
Aromatic *o*-diamines
o-aminophenols
Catalytic constant
Michaelis constant

ABSTRACT

The kinetics of tyrosinase acting on *o*-aminophenols and aromatic amines as substrates was studied. The catalytic constants of aromatic monoamines and *o*-diamines were both low, these results are consistent with our previous mechanism in which the slow step is the transfer of a proton by a hydroxyl to the peroxide in oxy-tyrosinase (Fenoll et al., Biochem. J. 380 (2004) 643–650). In the case of *o*-aminophenols, the hydroxyl group indirectly cooperates in the transfer of the proton and consequently the catalytic constants in the action of tyrosinase on these compounds are higher. In the case of aromatic monoamines, the Michaelis constants are of the same order of magnitude than for monophenols, which suggests that the monophenols bind better (higher binding constant) to the enzyme to facilitate the π–π interactions between the aromatic ring and a possible histidine of the active site. In the case of aromatic *o*-diamines, both the catalytic and Michaelis constants are low, the values of the catalytic constants being lower than those of the corresponding *o*-diphenols. The values of the Michaelis constants of the aromatic *o*-diamines are slightly lower than those of their corresponding *o*-diphenols, confirming that the aromatic *o*-diamines bind less well (lower binding constant) to the enzyme.

1. Introduction

Tyrosinase (TYR, EC 1.14.18.1) is a copper-containing enzyme widely distributed in nature. It catalyses two types of reactions: (a) the *ortho*-hydroxylation of monophenols to *o*-diphenols (monophenolase activity) and (b) the oxidation of *o*-diphenols to *o*-quinones (diphenolase activity). Both types of reaction require molecular oxygen as the second substrate of the enzyme [2,3].

The catalytic centre of tyrosinase possesses a binuclear copper similar to that of hemocyanin and catechol oxidase [3]. The catalytic cycle of tyrosinase has three enzymatic forms: E_m (met-tyrosinase) with the copper as $Cu^{2+}Cu^{2+}$, E_d (deoxy-tyrosinase) with the copper as $Cu^{+}Cu^{+}$ and E_{ox} (oxy-tyrosinase) with copper in the form $Cu^{2+}Cu^{2+}O_2^{2-}$ [4]. In the structures of hemocyanin [3,5], catechol oxidase [6] and tyrosinase from *Streptomyces castaneoglobisporus* [7] and from *Bacillus megaterium* [8,9], each copper ion is coordinated by three histidines.

Apart from its natural substrates (monophenols and *o*-diphenols), tyrosinase is also capable of oxidising a variety of aromatic monoamines and *o*-aminophenols, such as 4-aminotoluene, or several aminophenolic derivatives of benzoic acid, such as 3-amino-4-hydroxybenzoic acid, 4-amino-3-hydroxybenzoic acid and 3,4-diaminobenzoic acid [10]. The source of tyrosinase used by these authors [10] was *Neurospora crassa*. Moreover, 3-hydroxyanthranilic acid has been shown to act as an activator of the monophenolase activity of mushroom tyrosinase [11], reducing the lag period for reactions with non-cyclising phenolic substrates (4-*tert*-butylphenol/4-*tert*-butylcatechol). In another report, the same authors described the oxidation of 3-hydroxykynurenine, a tryptophan catabolite, by mushroom tyrosinase [12]. On the other hand, 3-amino-L-tyrosine has been described as a potent competitive inhibitor of the monophenolase activity and does not serve as a substrate. It was proposed that this aminophenol acts as a complexing agent of the copper ions in the *oxy* form of tyrosinase [13].

In a recent work [14], the interaction of mushroom tyrosinase with several aromatic monoamines, *o*-diamines and *o*-aminophenols was described using different spectrophotometric and oxymetric techniques. Consequently, 3-amino-L-tyrosine was shown to be a real substrate of tyrosinase, contrary to the findings published by Maddaluno and Faull [13].

In all the works above [11–14], *o*-aminophenols and aromatic monoamines and *o*-diamines were seen to act as substrates of tyrosinase because they are all structural analogues of the natural substrates of the enzyme (*o*-diphenols and monophenols).

The kinetic characterisation of aromatic monoamines, *o*-diamines and *o*-aminophenols is difficult because the product of the reaction, *o*-quinoneimine, is unstable [10,11]. Kinetic studies have been carried out using oxymetric techniques, which have provided quantitative

* Corresponding author. Tel.: +34 868 884764; fax: +34 868 883963.
E-mail address: canovasf@um.es (F. Garcia-Canovas).

1570-9639/$ – see front matter © 2011 Elsevier B.V. All rights reserved.
doi:10.1016/j.bbapap.2011.07.015

information [10]. However, spectrophotometric techniques [10,14] do not provide such information because the product evolves. In a recent work [15], we presented a revision of the spectrophotometric techniques used for measuring tyrosinase activity. In the present work, we widen the use of these methods to the characterisation of the substrates above, applied especially to the case of *o*-aminophenols and aromatic *o*-diamines, using ascorbic acid, the concentration of which decays and is followed spectrophotometrically. We also study the possibility that some *o*-quinoneimines may give rise to an isosbestic point during their evolution. Oxymetric techniques have also been used [16], especially to characterise monophenols and aromatic amines, permitting kinetic parameters to be reliably obtained for this series of compounds.

Bearing in mind the above, the aim of this study was to take a deeper look at the tyrosinase mechanism, considering its action on several substrates: aromatic monoamines, *o*-diamines and *o*-aminophenols. The results obtained are compared to those obtained for *o*-diphenols and monophenols. Based on the findings, the mechanism of tyrosinase is discussed and the decisive steps of the catalysis are characterised.

2. Material and methods

2.1. Reagents

Mushroom tyrosinase (TYR, *o*-diphenol:O_2 oxidoreductase, EC 1.14.18.1) (1530 U/mg), was obtained from Sigma Chemical (St. Louis, MO). All substrates and L-ascorbic acid (AH_2) were obtained from Sigma Chemical (St. Louis, MO). Stock solutions of the reducing substrates were prepared in 0.15 mM phosphoric acid to prevent autooxidation. Milli-Q system (Millipore Corp.) ultrapure water was used throughout this research. The buffer used was 30 mM sodium phosphate (pH 7.0).

2.2. Enzyme source

Tyrosinase (1530 U/mg; TYR) was purified according to [17]. Protein concentration was determined by Bradford's method using bovine serum albumin as standard [18].

2.3. Spectrophotometric assays

Absorption spectra were recorded in a visible–ultraviolet Perkin-Elmer Lambda 35-spectrophotometer interfaced on-line with a PC compatible Intel-Pentium microcomputer, at a scanning speed of 60 nm/s controlled by the UV-Winlab software. The temperature was maintained at 25 °C using a Haake D16 circulating water bath with a heater/cooler, and checked using a Cole-Parmer digital thermometer with a precision of 0.1 °C. Kinetic assays were also carried out with the instruments above, monitoring AH_2 disappearance (2,3-diaminobenzoic acid, 3,4-diaminotoluene, 4-methoxy-1,2-phenylendiamine, 4-amino-3-hydroxybenzoic acid, 3-amino-L-tyrosine, 2-aminophenol and 3-methylcatechol), NADH disappearance (catechol), the formation of dopachrome (L-tyrosine and L-dopa), the appearance of an adduct between *o*-quinoneimine and substrate (2-aminobenzoic acid, 3-aminotoluene, 4-aminotoluene, 2,3-diaminotoluene, 1,2-diaminobenzene, 2-amino-3-hydroxybenozic acid, 3-amino-4-hydroxybenzoic acid, 3-amino-4-hydroxytoluene, 4-amino-3-hydroxytoluene, 3-hydroxytoluene, 2-hydroxyanisole, 4-methylcatechol and 3-methoxycatechol) or the appearance of an adduct between MBTH, a nucleophile reagent, and the substrate (4-aminoanisole, 4-aminophenylalanine and 4-hydroxyanisole). The measuring wavelength (λ) and the molar absorbtivity coefficient (ε) for each substrate are summarised in Table 1SM (Supplementary material). The cuvettes (final volume of 1 mL) contained 30 mM sodium phosphate buffer (pH 7.0) and O_2 at a concentration which saturates the corresponding enzymes [19]. The substrate concentration was varied as indicated in each figure legend, and the reaction was started by adding enzyme (TYR). The coupled reagent concentration (AH_2, NADH or MBTH) is indicated in each figure legend.

2.4. Oxymetric assays

Oxygen consumption was measured with a Clark-type electrode coupled to a Hansatech Oxygraph (King's Lynn, Norfolk, UK). The equipment was calibrated using the TYR/4-*tert*-butylcatechol method [16]. Nitrogen was bubbled through the reaction medium to remove the oxygen when necessary. The cuvette (final volume 2 mL) contained 30 mM sodium phosphate buffer (pH 7.0) and the substrate concentration was varied. In every case, AH_2 was added to the medium to maintain the substrate concentration constant. The reaction was started by adding substrate. The medium was stirred constantly and the temperature was kept at 25 ± 0.1 °C using a Haake D16 circulating water-bath. The substrates characterised by this method were: 3-aminobenzoic acid, 4-aminobenzoic acid, 2-aminotoluene, 2-aminoanisole, 3-aminoanisole, aniline, 3,4-diaminobenzoic acid, 3-amino-2-hydroxybenzoic acid, 2-hydroxybenzoic acid, 3-hydroxybenzoic acid, 4-hydroxybenzoic acid, 2-methylphenol (*o*-cresol), 4-methylphenol (*p*-cresol), 3-hydroxyanisole, phenol, 2,3-dihydroxybenzoic acid and 3,4-dihydroxybenzoic acid. In the cases of aromatic monoamines and monophenols, the corresponding *o*-diphenol or 4-*tert*-butylcatechol (when the corresponding *o*-aminophenols or *o*-diphenol was not available commercially, e.g. 2-aminotoluene, 2-aminoanisole and 3-aminoanisole) were added to the medium to avoid the lag phase of the monophenolase activity of tyrosinase ($[D]_{ss}/[M]_{ss} = R$) [20].

2.5. Kinetic analysis

For TYR, the initial rate values (V_0) were calculated from triplicate measurements at each reducing substrate concentration, and V_0*vs.* $[S]_0$ data were adjusted to the Michaelis–Menten equation [Eq. (1)] through the Sigma Plot 9.0 program for Windows [21], obtaining the maximum rate (V_{max}) and Michaelis constant for each substrate (K_m). From these values and according to Eq. (2), the catalytic constant (k_{cat}) can be calculated.

3. Results and discussion

In recent years much effort has been dedicated to the kinetics of the action mechanism of tyrosinase acting on its physiological substrates, monophenols and *o*-diphenols [2,3,22–24]. Besides these physiological substrates, other types of non-phenolic substrate, such as NADH [25], ascorbic acid [26], tetrahydropterines or tetrahydrofolic acid [27,28], have been characterised. Moreover, to characterise kinetically aromatic monoamines and *o*-diamines and *o*-aminophenols, several oxymetric and spectrophotometric measuring methods have been designed [15].

3.1. Oxymetric methods

Generally speaking, all substrates of tyrosinase can be characterised according to their consumption of oxygen, although, due to the low activity shown by the enzyme towards some of them, such as aromatic monoamines and *o*-diamines and *o*-aminophenols, spectrophotometric methods are preferred, especially when the disappearance of a coupled reagent with a high coefficient of molar absorptivity can be measured.

3.2. Spectrophotometric methods

When possible, ascorbic acid (AH_2) was used, since it reduces the *o*-quinoneimine or *o*-diimine to the corresponding *o*-aminophenol or aromatic *o*-diamine, respectively. When the spectrum of the substrate overlaps that of the AH_2, a problem arises with the saturation of the

phototube. In this case, the oxymetric method is used or, if possible, depending on the substrate, the visible zone is measured, taking advantage of the formation of adducts between the *o*-quinoneimine and the substrate (Scheme 1), or between the *o*-quinoneimine and a coupled/bound reagent, such as MBTH.

3.3. Oxidation of o-aminophenols and aromatic o-diamines by periodate in deficiency

The oxidation of *o*-aminophenols and aromatic *o*-diamines by periodate in deficiency gives rise to the formation of *o*-quinoneimine (Scheme 1), which suffers a nucleophilic attack on the part of the amino group of the substrate, originating an adduct which is oxidised again by another molecule of *o*-quinoneimine. The new quinone suffers a nucleophilic attack, giving rise to a new leuco compound, which, in turn, is oxidised by another molecule of *o*-quinoneimine to form a *p*-quinone. Fig. 1 depicts the appearance of an isosbestic point during the evolution of the *o*-quinoneimine as a result of the oxidation of 3-hydroxyantrhanilic acid by periodate in deficiency. Note that a stoichiometry of 3 *o*-quinoneimine/1 *p*-quinoneimine is accomplished. The existence of an isosbestic point permits the oxidation of 3-hydroxyanthranilic acid to be followed at this wavelength.

3.4. Formation of chromophoric adducts with MBTH

In order to study the characteristics of the MBTH-*o*-quinoneimine adducts, the oxidation of various aromatic monoamines by O_2 catalysed by tyrosinase was carried out in the presence of MBTH (Fig. 2). The pigment formed with 4-aminophenylalanine and 4-aminoanisole had an absorbance maximum which ranged from 497 to 498 nm (Table 1SM). The pH affected the solubility and stability of the adducts. The solubilisation of these compounds was achieved by adding 2% (v/v) dimethylformamide (DMF) to the reaction medium [29]. At pH 7.0, the adducts were unstable but showed an isosbestic point. The MBTH is a potent nucleophile through its amino group, which shows different degrees of protonation–deprotonation, depending on the pH. The ionisation constant for this group was determined by both potentiometric and spectrophotometric methods ($pK = 5.8 \pm 0.4$) [29]. Depending on its stability, each *o*-quinoneimine needs a different $[MBTH]_{sat}$ to complete the formation of the adduct (see the legends of the figures).

3.5. Oxidation of o-aminophenols by TYR and comparison with o-diphenols

We studied the oxidation of several *o*-aminophenols by mushroom tyrosinase using different measuring methods (see Supplementary material), which enabled us to characterise kinetically these substrates (Table 1).

Fig. 1 depicts the oxidation of 3-hydroxyanthranilic acid (2-amino-3-hydroxybenzoic acid) by periodate in deficiency measuring the gradual appearance of the product. An adduct is formed between the

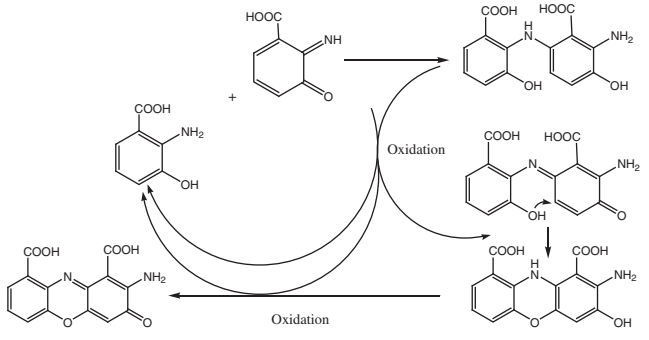

Scheme 1. Mechanism for evolution of 3-hydroxyanthranilic acid´s *o*-quinoneimine in the presence of an excess of *o*-aminophenol.

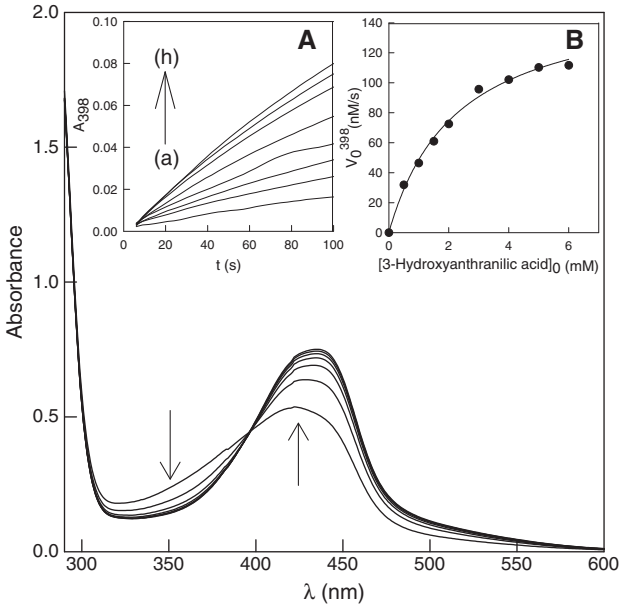

Fig. 1. Spectrophotometric scans of the 3-hydroxyanthranilic acid oxidation by periodate in deficiency. The experimental conditions were 30 mM sodium phosphate buffer (pH 7.0), 25 °C, initial concentrations of 3-hydroxyanthranilic acid and periodate, $[3\text{-hydroxyanthranilic acid}]_0$ and $[IO_4^-]_0$, were 0.6 mM and 60 μM, respectively. The spectrophotometric scans were made every 3 min. Inset A. Spectrophotometric recordings of the oxidation of 3-hydroxyanthranilic acid by TYR at a wavelength of 398 nm. The experimental conditions were 30 mM sodium phosphate buffer (pH 7.0), 25 °C, initial concentration of enzyme, $[E]_0$, was 0.61 μM and the initial substrate concentrations (mM) were: (a) 0.5, (b) 1, (c) 1.5, (d) 2, (e) 3, (f) 4, (g) 5 and (h) 6. Inset B. Representation of the steady-states rates (V_0) *vs.* $[3\text{-hydroxyanthranilic acid}]_0$.

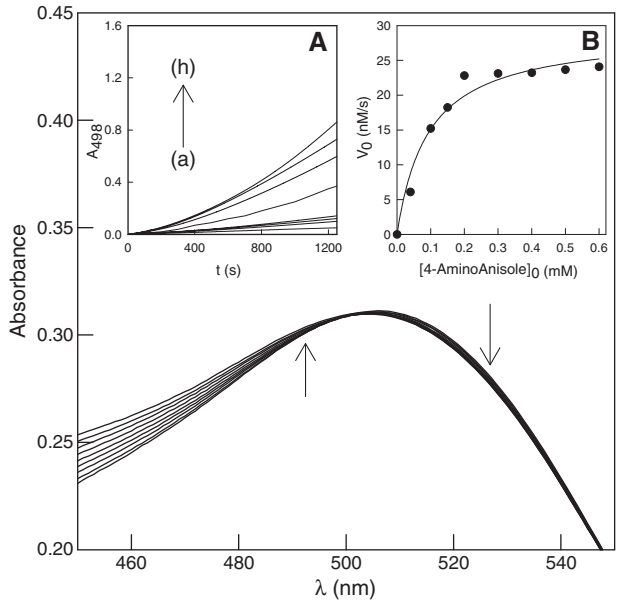

Fig. 2. Spectrophotometric scans of the 4-aminoanisole oxidation by TYR in the presence of MBTH. The experimental conditions were 30 mM sodium phosphate buffer (pH 7.0), 25 °C, $[4\text{-aminoanisole}]_0 = 0.5$ mM, $[E]_0 = 0.9$ μM, $[MBTH]_0 = 2.5$ mM and $[DMF]_0 = 2\%$. The spectrophotometric scans were made every 15 min. Inset A. Spectrophotometric recordings of the oxidation of 4-aminoanisole by TYR at a wavelength of 498 nm. The experimental conditions were 30 mM sodium phosphate buffer (pH 7.0), 25 °C, $[E]_0 = 10$ nM, initial concentration of MBTH and DMF, $[MBTH]_0$ and $[DMF]_0$, were 2.5 mM and 2%, respectively and the initial substrate concentrations (mM) were (a) 0.05, (b) 0.1, (c) 0.15, (d) 0.2, (e)0.3, (f) 0.4, (g) 0.5 and (h) 0.6. Inset B. Representation of the initial steady-state rates (V_0) *vs.* $[4\text{-aminoanisole}]_0$. The experimental conditions are the same as in Fig. 2.

Table 1
Values of the kinetic constants characterising the oxidation of aminophenols and diphenols by TYR.

Aminophenols	k_{cat} (s^{-1})	K_m (mM)	Diphenols	k_{cat} (s^{-1})	K_m (mM)
2-amino-3-hydroxybenzoic acid	0.13 ± 0.01	2.27 ± 0.22	2,3-dihydroxybenzoic acid	0.37 ± 0.04	1.02 ± 0.12
3-amino-2-hydroxybenzoic acid	0.13 ± 0.01	0.36 ± 0.04			
3-amino-4-hydroxybenzoic acid	0.45 ± 0.01	0.11 ± 0.01	3,4-dihydroxybenzoic acid	8.11 ± 0.31	0.07 ± 0.01
4-amino-3-hydroxybenzoic acid	0.50 ± 0.01	0.15 ± 0.01			
3-amino-4-hydroxytoluene	29.42 ± 1.58	2.73 ± 0.56	4-methylcatechol	842.12 ± 26.11	0.10 ± 0.01
4-amino-3-hydroxytoluene	26.12 ± 2.13	2.36 ± 0.43			
3-amino-L-tyrosine	1.35 ± 0.15	0.90 ± 0.18	L-dopa	102.62 ± 19.21	0.55 ± 0.08
2-aminophenol	60.57 ± 2.84	0.78 ± 0.08	Catechol	874.10 ± 30.21	0.16 ± 0.01

substrate and product of the reaction. This adduct is rapidly oxidised to form cinnabarinic acid, giving rise to an isosbestic point at 398 nm [10,11]. Fig. 1 inset A shows the experimental recordings of the oxidation of different initial concentrations of 3-hydroxyanthranilic acid, $[S]_0$, by TYR. The initial rates of these oxidation processes with respect to $[S]_0$ are shown in Fig. 1 inset B. Non-linear regression gives V_{max} and K_m according to the equation:

$$V_0 = \frac{V_{max}[S]_0}{K_m + [S]_0} \quad (1)$$

where:

$$V_{max} = 2k_{cat}[E]_0 \quad (2)$$

and

$$K_m = \frac{k_{cat}}{k_6} \quad (3)$$

k_{cat} being the catalytic constant, $[E]_0$ the initial enzyme concentration and k_6 the substrate binding constant to the form oxy-tyrosinase.

In the case of 2-aminophenol, as shown in Fig. 3, ascorbic acid (AH_2) was used as reductant. In order to choose the most suitable wavelength for the measurement, we first obtained the absorption spectra of AH_2 (recording a, Fig. 3) and of 2-aminophenol (recording b, Fig. 3), choosing in this case 265 nm, which represents the absorption maximum of AH_2 ($\varepsilon = 11170\ M^{-1}\ cm^{-1}$) [30]. Fig. 3, Inset A depicts the experimental recordings of the gradual disappearance of AH_2. Fig. 3, Inset B shows the initial rates of TYR *vs.* $[2\text{-aminophenol}]_0$. Non-linear-fitting of the values of V_0, in accordance with Eq. (1), gives V_{max} and K_m (see Table 1). In the case of 3-amino-2-hydroxybenzoic acid (3-aminosalicylic acid), the consumption of oxygen was measured (see Table 1).

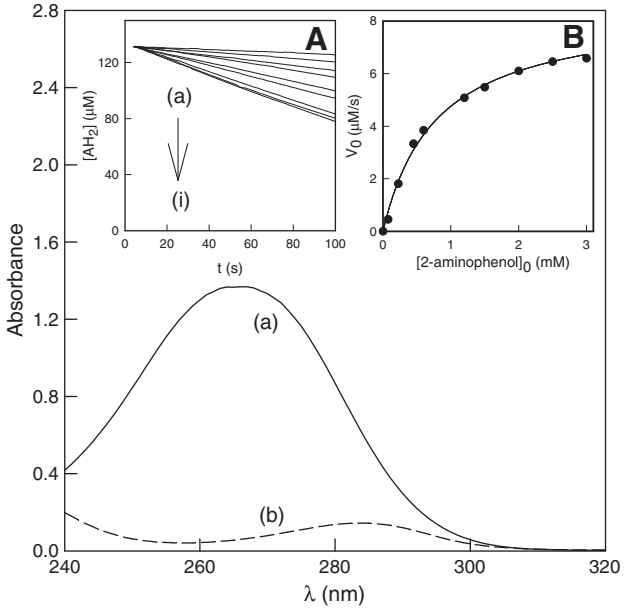

Fig. 3. Spectrophotometric scan of the 2-aminophenol and AH_2. The experimental conditions were 30 mM sodium phosphate buffer (pH 7.0), 25 °C, initial concentration of ascorbic acid and 2-aminophenol, $[AH_2]_0$ and $[2\text{-aminophenol}]_0$, were 0.12 mM (a) and 0.6 mM (b), respectively. Inset A. Spectrophotometric recordings of the 2-aminophenol oxidation by TYR at a wavelength of 265 nm. The experimental conditions were 30 mM sodium phosphate buffer (pH 7.0), 25 °C, $[AH_2]_0 = 0.13$ mM and $[E]_0 = 60$ nM and the initial substrate concentrations (mM) were: (a) 0.075, (b) 0.225, (c) 0.45, (d) 0.6, (e) 1.2, (f) 1.5, (g) 2, (h) 2.5 and (i) 3. Inset B. Representation of the initial steady-state rates (V_0) *vs.* $[2\text{-aminophenol}]_0$.

Table 1 shows the kinetic constants obtained for the different substrates and, where possible, these are compared with those obtained for the corresponding *o*-diphenols. Note how the *o*-aminophenols have the same or similar k_{cat} values when positions 2 and 3 or 3 and 4 are compared for the amino or hydroxyl group; for example, the value of k_{cat} for 2-amino-3-hydroxybenzoic acid is approximately the same as that of 2-hydroxy-3-aminobenzoic acid ($0.13 \pm 0.01\ s^{-1}$) and the k_{cat} of 3-amino-4-hydroxybenzoic acid is approximately the same as that of 3-hydroxy-4-aminobenzoic acid (Table 1). The catalytic constant increases from the *ortho*/*meta* position to the *meta*/*para* position and the same occurs if the substituent in C-1 is an electrodonating (—CH_3) or electrowithdrawing (—COOH) group. A similar situation exists for *o*-diphenols (see Table 1). The same applies when a chain exists in C-1, as in the case of 3-amino-L-tyrosine and L-dopa, while the values of k_{cat} are much lower than in the case of 2-aminophenol and catechol.

The Michaelis constants (see Table 1) and Eq. (3) are related with the catalytic constants and, in the case of *o*-aminophenols, which have low k_{cat} values, the K_m values are also low. Note that the *ortho* position of the amino group of 2-amino-3-hydroxybenzoic acid has a higher K_m, which, according to Eq. (3), indicates that its binding constant k_6 is lower than that of 3-amino-2-hydroxybenzoic acid, which might be explained by the steric hindrance of the amino group *ortho* position. The corresponding *o*-diphenol (2,3-dihydroxybenzoic acid) has a lower K_m value than 2-amino-3-hydroxybenzoic acid but it is three times higher than the value corresponding to 2-hydroxy-3-aminobenzoic acid, which agrees with the higher k_{cat}. In the case of 3-amino-4-hydroxybenzoic acid and 3-hydroxy-4-aminobenzoic acid, their values are similar to that of 3,4-dihydroxybenzoic acid (Table 1). The K_m values of 3-amino-4-hydroxytoluene and 3-hydroxy-4-aminotoluene (2.73 ± 0.56 and 2.36 ± 0.43 mM, respectively) are almost identical but, because the k_{cat} is higher than in the case above, the K_m is also higher. When these values are compared with those of their corresponding *o*-diphenols (Table 1), the values of k_{cat} are much lower in the case of *o*-aminophenols and the K_m values are in the same range, meaning that the *o*-diphenols bind better to the enzyme (higher k_6). The binding of the *o*-diphenols to the enzyme may be more favoured than in the case of the *o*-aminophenols because the π–π interaction between the substrate and a possible histidine of the active site is favoured in the case of *o*-diphenols and hindered in the case of aminophenols (Table 1).

If an electrodonating group exists on C-1, the benzene ring will be more electron-dense, binding will be less strong (due to the greater repulsion between the rings) and therefore, the k_6 value will be lower since the π–π interactions are hindered. If an electrowithdrawing

Table 2
Values of the kinetic constants characterising the oxidation of aromatic diamines and *o*-diphenols by TYR.

Aromatic diamines	k_{cat} (s^{-1})	K_m (mM)	Diphenols	k_{cat} (s^{-1})	K_m (mM)
2,3-diaminobenzoic acid	0.05 ± 0.01	0.28 ± 0.04	2,3-dihydroxybenzoic acid	0.37 ± 0.04	1.02 ± 0.12
3,4-diaminobenzoic acid	0.08 ± 0.01	0.15 ± 0.02	3,4-dihydroxybenzoic acid	8.11 ± 0.31	0.07 ± 0.01
2,3-diaminotoluene	0.11 ± 0.01	0.96 ± 0.11	3-methyl Catechol	104.2 ± 4.7	1.10 ± 0.14
3,4-diaminotoluene	0.51 ± 0.04	0.06 ± 0.01	4-methyl Catechol	842.12 ± 26.11	0.10 ± 0.01
4-methoxy-1,2-phenylendiamine	1.51 ± 0.13	0.36 ± 0.05	3-methoxycatechol	17.83 ± 0.53	1.26 ± 0.13
1,2-diaminobenzene	0.53 ± 0.05	0.46 ± 0.05	Catechol	874.10 ± 30.21	0.16 ± 0.01

group exists on C-1 the benzene ring will be of lower electron density, which will result in better substrate binding (higher k_6).

3.6. Oxidation of aromatic *o*-diamines by TYR and comparison with their respective *o*-diphenols

Table 2 shows the results obtained when the oxidation of aromatic *o*-diamines was studied. The values of the catalytic constants of the aromatic *o*-diamines are low, the 2,3-diamines having, as expected, a lower k_{cat} than the *o*-diamines substituted in 3,4. Furthermore, if the molecule in C-1 has an electrowithdrawing group, the values of k_{cat} are lower than when an electrodonating group is present. The same applies in the case of *o*-diphenols, although the catalytic constants are greater than in the case of the corresponding aromatic *o*-diamines.

The values of K_m are greater in the case of substrates with their substituents in *ortho* position with respect to C-1 and, in general, fulfil Eq. (3). Although the k_{cat} values of the *o*-diphenols are much greater than those of the aromatic *o*-diamines, the value of the binding constant (k_6) to the form E_{ox} must be high, so that, according to Eq. (3), the K_m values must be in the same range as those of the aromatic *o*-diamines. A possible explanation for this is that, in the case of *o*-diphenols, π–π interactions between the aromatic ring and a possible histidine of the active site are favoured.

Fig. 4 shows the recordings of the oxidation of 3,4-diaminobenzoic acid by TYR and Fig. 4 inset shows the values of V_0*vs.* the initial concentration of 3,4-diaminobenzoic acid, [3,4-diaminobenzoic acid]$_0$, which enables V_{max} and K_m to be calculated, by means of Eq. (1).

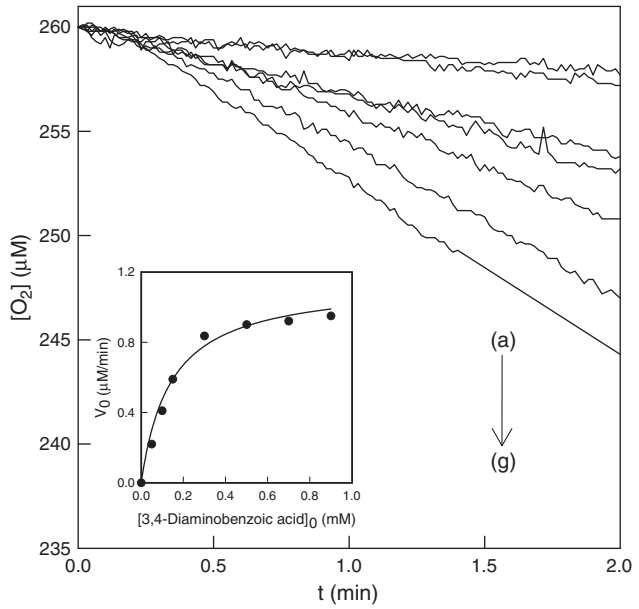

Fig. 4. Oxymetric recordings of the oxidation of 3,4-diaminobenzoic acid by TYR. The experimental conditions were 30 mM sodium phosphate buffer (pH 7.0), 25 °C, $[AH_2]_0 = 0.2$ mM, $[E]_0 = 0.25$ μM and the initial substrate concentrations (mM) were: (a) 0.05, (b) 0.1, (c) 0.15, (d) 0.3, (e) 10.5, (f) 0.7 and (g) 0.9. Inset. Representation of the initial steady-state rates (V_0) *vs.* [3,4-diaminobenzoic acid]$_0$.

3.7. Oxidation of aromatic monoamines by TYR and comparison with monophenols

TYR oxidises *o*-diphenols to *o*-quinones because of its diphenolase or catecholase activity. However, it also shows monophenolase or cresolase, whereby it hydroxylates monophenols to *o*-diphenols. In the same way as it oxidises *o*-aminophenols and aromatic *o*-diamines to their corresponding *o*-quinoneimine and diimines, TYR can also hydroxylate aromatic monoamines and convert them into *o*-aminophenols and *o*-quinoneimines. Using the measuring methods described in this study, the hydroxylation of several aromatic monoamines with different groups in their side chains (in C-1) was characterised.

Fig. 5 depicts how the oxidation of 3-amino-4-hydroxytoluene by periodate in deficiency gives rise to an isosbestic point at λ = 318 nm. Fig. 5 inset A shows the spectrophotometric recordings at 318 nm, obtained by measuring the appearance of oxidised adduct. Raising the initial concentration of 3-aminotoluene (the aromatic monoamine corresponding to 3-amino-4-hydroxytoluene) increases the reaction rate, and when these initial rates are represented with respect to [S]$_0$ and fitted by non-linear regression to Eq. (1), V_{max} and K_m can be obtained for this aromatic monoamine, as shown in Fig. 5 inset B (see Table 2).

The oxidation of 4-aminoanisole by tyrosinase in the presence of MBTH gives an isosbestic point at λ = 498 nm (Fig. 2), which permits the molar absorptivity (ε) to be calculated at this point. Fig. 2 inset A

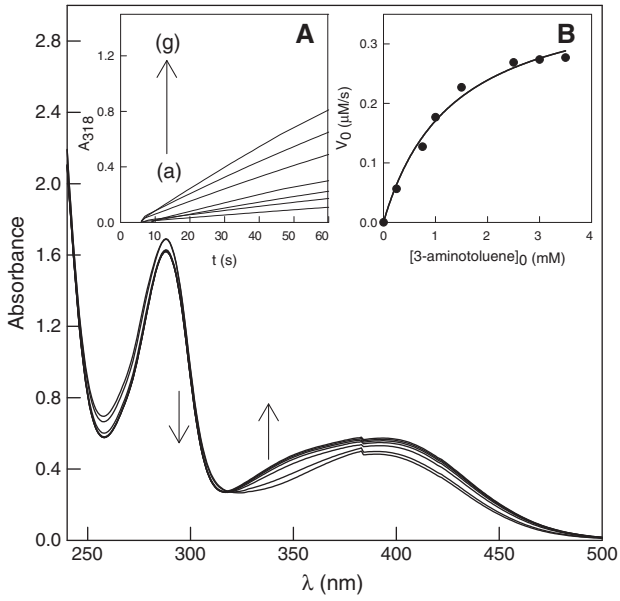

Fig. 5. Spectrophotometric scans of the 3-amino-4-hydroxytoluene oxidation by periodate in deficiency. The experimental conditions were 30 mM sodium phosphate buffer (pH 7.0), 25 °C, $[3\text{-amino-4-hydroxytoluene}]_0 = 0.6$ mM and $[IO_4^-]_0 = 60$ μM. The spectrophotometric scans were made every 3 min. Inset A. Spectrophotometric recordings of the oxidation of 3-aminotoluene by TYR at a wavelength of 318 nm. The experimental conditions were 30 mM sodium phosphate buffer (pH 7.0), 25 °C, $[E]_0 = 0.45$ μM and the initial substrate concentrations (mM) were: (a) 0.25, (b) 0.75, (c) 1.0, (d) 1.5, (e) 2.5, (f) 3 and (g) 3.5. Inset B. Representation of the initial steady-state rates (V_0) *vs.* [3-aminotoluene]$_0$.

Table 3
Values of the kinetic constants characterising the oxidation of aromatic monoamines and monophenols by TYR.

Aromatic monoamines	k_{cat} (s^{-1})	K_m (mM)	Phenols	k_{cat} (s^{-1})	K_m (mM)
Aniline	0.45 ± 0.03	0.64 ± 0.09	Phenol	10.81 ± 1.51	0.61 ± 0.04
2-aminobenzoic acid	$(0.13 \pm 0.01) \times 10^{-3}$	2.36 ± 0.34	2-hydroxybenzoic acid	0.046 ± 0.002	2.62 ± 0.18
3-aminobenzoic acid	$(0.33 \pm 0.01) \times 10^{-3}$	0.28 ± 0.02	3-hydroxybenzoic acid	0.64 ± 0.03	2.35 ± 0.32
4-aminobenzoic acid	$(5.04 \pm 0.32) \times 10^{-3}$	0.14 ± 0.01	4-hydroxybenzoic acid	1.70 ± 0.07	0.22 ± 0.03
2-aminotoluene	0.33 ± 0.02	2.93 ± 0.38	2-methylphenol	7.37 ± 0.40	1.48 ± 0.18
3-aminotoluene	0.46 ± 0.04	1.26 ± 0.07	3-methylphenol	7.51 ± 0.65	0.62 ± 0.09
4-aminotoluene	1.01 ± 0.03	1.04 ± 0.12	4-methylphenol	16.12 ± 1.53	0.38 ± 0.05
2-aminoanisole	0.09 ± 0.01	0.26 ± 0.03	2-hydroxyanisole	5.47 ± 0.21	5.40 ± 0.60
3-aminoanisole	0.12 ± 0.01	0.15 ± 0.02	3-hydroxyanisole	46.87 ± 2.06	2.53 ± 0.26
4-aminoanisole	1.24 ± 0.21	0.09 ± 0.01	4-hydroxyanisole	184.20 ± 6.10	0.08 ± 0.01
4-aminophenylalanine	0.01 ± 0.01	0.42 ± 0.05	4-hydroxyphenylalanine	8.12 ± 1.44	0.27 ± 0.03

depicts the oxidation of 4-aminoanisole by TYR, measuring the appearance of oxidised adduct formed between the *o*-quinoneimine and a powerful nucleophile like MBTH [15,29]. By representing V_0*vs.* $[S]_0$ (Fig. 2 inset B), V_{max} and K_m can be calculated by non-linear regression fitting with respect to Eq. (1) (Table 3).

As in the case of monophenols, the natural substrates of TYR, aromatic monoamines, have very low catalytic constants compared with *o*-aminophenols, although the constants are higher in aromatic monoamines with electrodonating groups or with H in their side chain on C-1 than in those with electrowithdrawing groups. When aromatic monoamines substituted in 2, 3 or 4 position of the benzene ring are compared, those with the amino group in 4 show a higher k_{cat}, suggesting that the enzyme hydroxylates substrates substituted in *para* position more readily than those substituted in *meta* and *ortho* positions because of the lower steric hindrance [31] (Table 3).

The Michaelis constants (K_m) follow the order *ortho*>*meta*>*para* for both aromatic monoamines and phenols and, moreover, fulfil Eq. (3). Note the very little difference that frequently exists between the Michaelis constants of the aromatic monoamines and *o*-diamines (Tables 2 and 3).

3.8. Proposed mechanisms for the oxidation of aromatic monoamines and o-diamines and aminophenols by TYR

Schemes 2 and 3 represent the proposed structural mechanism to explain the oxidation of aromatic monoamines and *o*-diamines and *o*-aminophenols by TYR. Scheme 2 refers to the oxidation of *o*-aminophenols (diphenolase activity) and aromatic monoamines (monophenolase activity). Starting with the enzymatic form E_m, its binding to the *o*-aminophenol in Step 1 is seen to form the complex $(E_m-S)_0$. Once bound to the substrate, a proton from the NH_2 group is transferred to a group of the enzyme, which acts as a base, and then the nitrogen of the substrate binds to the *CuB* of the active site of the enzyme, forming the complex $(E_m-S)_1$. The amino group of the substrate is always the first to bind because it has a greater nucleophilic power than the hydroxyl (Step 2). In Step 3, the hydroxyl group transfers a proton to a histidine of the *CuA* of the enzyme active site [7]. The *o*-aminophenol is thus bound diaxially to the enzyme and the concerted oxidation/reduction generates the quinoneimine and the deoxygenated form of the enzyme E_d (Step 4). In Step 5, this form, E_d, binds to O_2 to form E_{ox}, while in Step 6, another molecule of the substrate (*o*-aminophenol) binds to the enzyme $(E_{ox}-S)_0$. Then, the nitrogen from the substrate binds to *CuB* of the enzyme because it is a more potent nucleophile than the oxygen of the hydroxyl, giving $(E_{ox}-S)_1$; subsequently, the oxygen from the OH attacks the copper and the hydrogen is transferred to the histidine $(E_{ox}-S)_2$ (Step 7). The electrowithdrawing effect of the *CuB* may facilitate the transfer of the proton from the amino group to the peroxide group of the active site, since the base is already protonated $(E_{ox}-S)_3$. (Step 8). Since the *o*-aminophenol is bound diaxially to E_{ox}, a concerted oxidation/reduction action gives rise to E_m and *o*-quinoneimine (Step 9), and the cycle starts again.

As regards the hydroxylation of the aromatic monoamines, as occurs with monophenols, the system starts with the form E_{ox} (Step 10) since the E_m form is inactive towards monophenols (Steps 16 and 17) and aromatic monoamines, which is the reason for the characteristic lag period of TYR [2,32,33]. The NH_2 group cedes the H^+ to the peroxide group of the active site of E_{ox}, while the remaining NH binds to the *CuB* of the enzyme (Step 11). Now the peroxide attacks the benzene ring, forming the complex $(E_m-A)_4$ (Step 12), which may undergo one of two possible reactions: (*i*) the NH group is protonated to become NH_2^+ (Step 13) and the complex $(E_m-S)_5$ is formed, while the binding of the oxygen to the copper of $(E_m-S)_5$ is broken, producing the complex $(E_m-S)_1$ (Step 15). This complex can yield $(E_m-S)_0$, releasing *o*-aminophenol or initiates the diphenolase cycle or (*ii*) the substrate is released from the enzyme by the OH group, forming the complex $(E_m-S)_2$ (Step 14), the rest of the cycle continuing as normal.

Note that, as with the monophenolase activity of TYR, which needs an *o*-diphenol to act, in the case of aromatic monoamines the presence of the *o*-aminophenol is necessary for the enzyme to act. This is formed in Steps 1 and 15 of Scheme 1.

As regards the aromatic *o*-diamines, the structural mechanism proposed (Scheme 3) is the same as that proposed for the *o*-aminophenols (Scheme 2) but, in this case, since two NH_2 groups exist, the NH_2 which attacks first will be that with a lower chemical shift (δ)—which, with electrodonating groups in C-1, will be the amino group in carbon 4 (δ_4).

4. Discussion on the kinetic constants of Tables 1–3

As a general commentary concerning Tables 1–3, the *o*-aminophenols and aromatic *o*-diamines are oxidised, while the aromatic monoamines are hydroxylated with catalytic constants that are much lower than those of the corresponding *o*-diphenols or monophenols.

In the case of *o*-aminophenols and *o*-diphenols (Table 1), the difference between the molecules with the same structure is one order of magnitude ($k_{cat}^{o-diphenols} > k_{cat}^{aminophenols}$). The similarity of the K_m values indicates, according to Eq. (3), that the *o*-diphenols bind

Scheme 2. Structural mechanism to explain the oxidation of *o*-aminophenols and aromatic monoamines by TYR. *Em*, met-tyrosinase; $(E_mS)_0$, met-tyrosinase/*o*-aminophenol complex; $(E_m–S)_1$, met-tyrosinase/*o*-aminophenol complex axially bound to a Cu atom; $(E_m–S)_2$, met-tyrosinase/*o*-aminophenol complex axially bound to a Cu atom with the proton transferred to the base B; $(E_m–S)_3$, met-tyrosinase/*o*-aminophenol complex axially bound to the two Cu atoms with the proton of the OH group transferred to the histidine; E_d, deoxy-tyrosinase; E_{ox}, oxy-tyrosinase; $(E_{ox}S)_0$, oxy-tyrosinase/*o*-aminophenol complex; $(E_{ox}–S)_1$, oxy-tyrosinase/*o*-aminophenol complex axially bound to a Cu atom; $(E_{ox}–S)_2$, oxy-tyrosinase/*o*-aminophenol complex axially bound to the two Cu atoms; $(E_{ox}–S)_3$, oxy-tyrosinase/*o*-aminophenol complex axially bound to the two Cu atoms with the proton transferred to the peroxide; $(E_{ox}A)_0$, oxy-tyrosinase/aromatic monoamine complex; $(E_{ox}A)_1$, oxy-tyrosinase/aromatic monoamine complex axially bound to a Cu atom with the proton transferred to the peroxide; $(E_m–S)_4$, met-tyrosinase/*o*-aminophenol complex axial-equatorially bound to the two Cu atoms; $(E_m–S)_5$, met-tyrosinase/*o*-aminophenol complex axial-equatorially bound to the two Cu atoms, binding to the base BH through a hydrogen bond; $(E_mA)_0$, met-tyrosinase/aromatic monoamine complex; $(E_mA)_1$, met-tyrosinase/aromatic monoamine complex axially bound to a Cu atom.

better to the enzyme (higher k_6) than the *o*-aminophenols, probably because a π–π interaction with a possible histidine is favoured. Note that the substituent in C-1 affects the values of k_{cat} and K_m—when the substituent is a methyl group (electrodonating), the k_{cat} for 3-hydroxy-4-aminotoluene or 3-amino-4-hydroxytoluene are high (slightly higher in the latter) and the K_m values, in accordance with

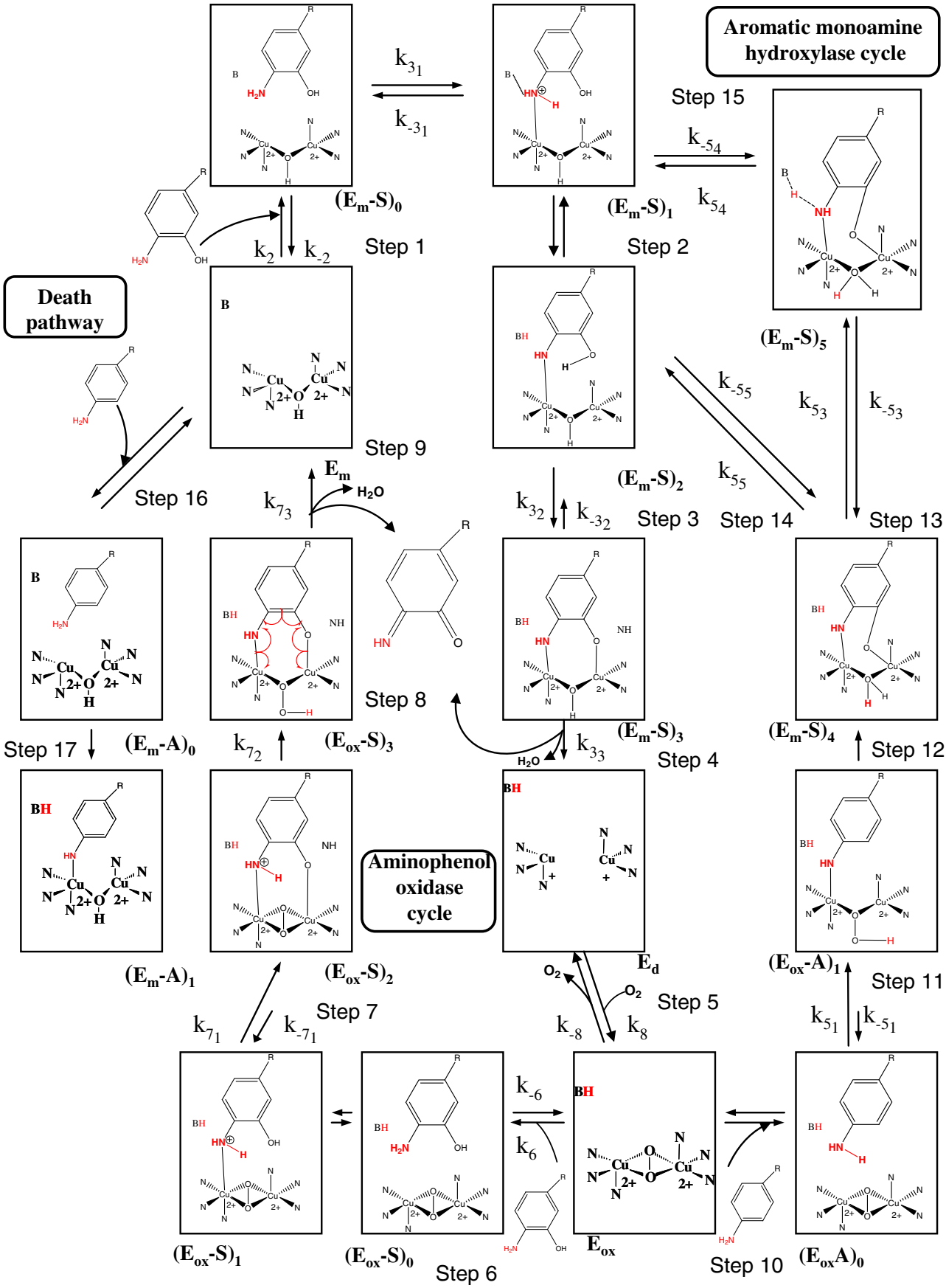

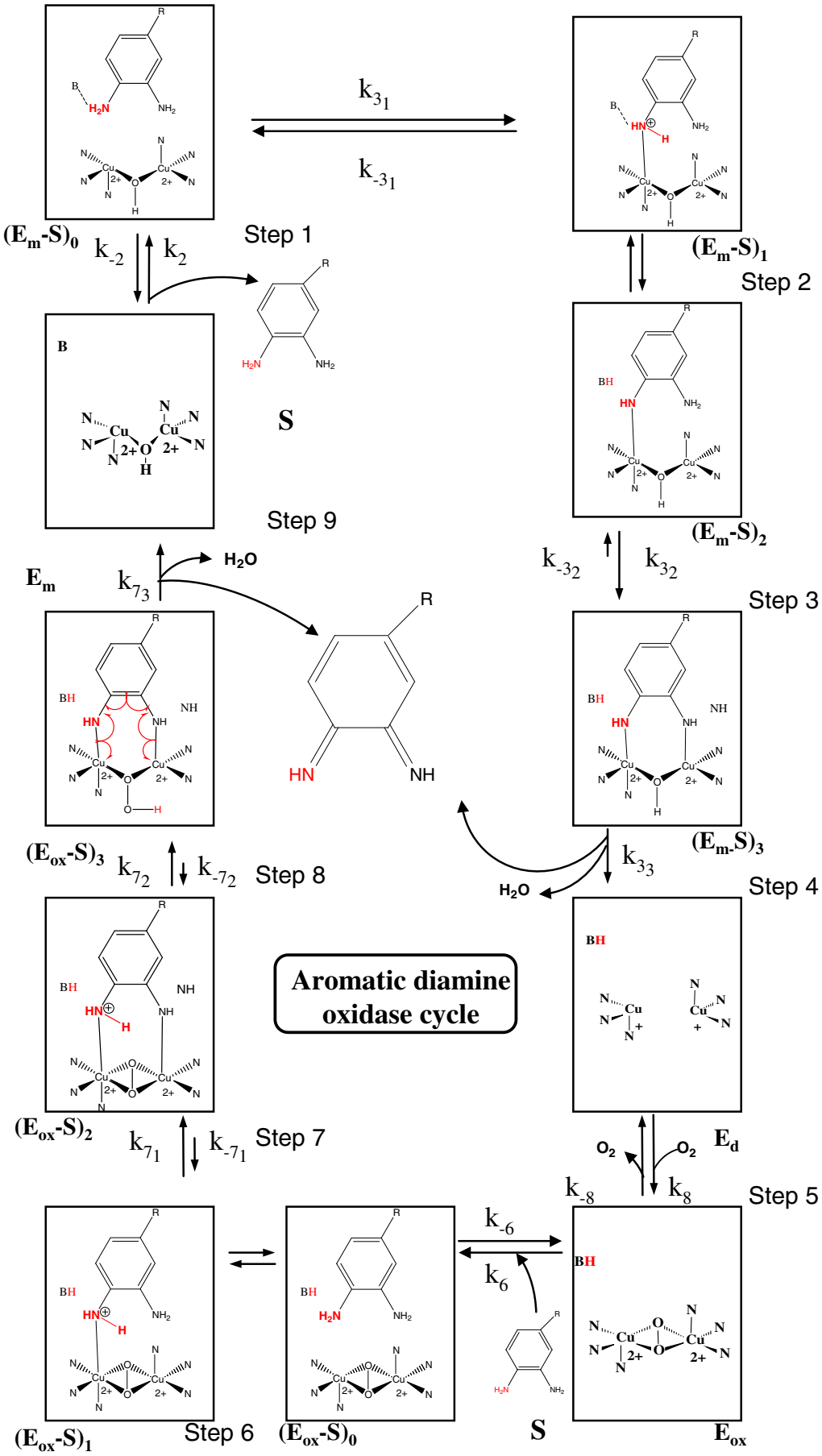
k_{3_1}
k_{-3_1}
$(E_m\text{-}S)_0$
Step 1
$(E_m\text{-}S)_1$
Step 2
k_{-2}
k_2
S
Step 9
$(E_m\text{-}S)_2$
k_{-3_2}
k_{3_2}
Step 3
E_m
k_{7_3}
H_2O
$(E_m\text{-}S)_3$
k_{7_2}
k_{-7_2}
Step 8
k_{3_3}
H_2O
Step 4
Aromatic diamine oxidase cycle
$(E_{ox}\text{-}S)_2$
k_{7_1}
k_{-7_1}
Step 7
O_2
O_2
E_d
k_{-8}
k_8
Step 5
k_{-6}
k_6
$(E_{ox}\text{-}S)_1$
Step 6
$(E_{ox}\text{-}S)_0$
S
E_{ox}

Eq. (3), increase (slightly more so in the case of 3-amino-4-hydroxytoluene). When an electrowithdrawing group exists on C-1 (such as a carboxyl group), the k_{cat} values fall (slightly more so for 3-amino-4-hydroxybenzoic acid), as do the K_m values (Table 2). Note that the k_{cat} is highest when there is no substituent in C-1 (see Table 2).

In the case of the aromatic *o*-diamines (Table 2), except 2,3-diaminobenzoic acid and 2,3-dihydroxybenzoic acid, in which steric hindrance phenomena dominate the process, the catalytic constants are two orders of magnitude lower than for their respective *o*-diphenols ($k_{cat}^{o-\,diphenols} \gg k_{cat}^{diamines}$). However, the K_m values are in the same range because the *o*-diphenols bind better to the enzyme than the aromatic *o*-diamines. When the amino group is in 2,3 position, the steric hindrance effect is greater than the electronic effect and the k_{cat} values fall, contrary to that which occurs with K_m.

Such behaviour is similar in the case of aromatic monoamines (Table 3). The values of the catalytic constants are two orders of magnitude greater than for the monophenols. Note that the k_{cat} values of the substrates with the group in *meta* position with respect to C-1 are always greater than those with the group in *ortho* position, since the steric hindrance is stronger than the electronic effect in *ortho*.

It has been demonstrated that TYR of *N. crassa* can oxidise several types of *o*-aminophenols and aromatic amines [10]. The same authors demonstrated the oxidation of these compounds using oxymetric methods, revealing also that the catalytic constants of TYR towards these compounds are three orders of magnitude lower than those of their phenolic analogues.

In a more recent work [11], mushroom TYR was demonstrated to oxidise an *o*-aminophenol substituted in 2 and 3 of the benzene ring, e.g. 3-hydroxy-2-aminobenzoic acid (3-hydroxyanthranilic acid, see Scheme 1), in the same way as *N. crassa* TYR. Similarly, the authors mention the influence of this compound on the monophenolase and diphenolase activities of mushroom TYR. A different type of effect was seen for *o*-aminophenol (3-hydroxykynurenine) on mushroom TYR, when it acted as a substrate/activator [12].

As in the case of *N. crassa* TYR, mushroom TYR shows catalytic constants that are two orders of magnitude lower for the oxidation of 2-aminobenzoic acid ($0.0001\ s^{-1}$) than for the oxidation of 2-hydroxybenzoic acid ($0.046\ s^{-1}$), the same being true for 4-aminoanisole ($1.24\ s^{-1}$) compared with 4-hydroxyanisole ($184.20\ s^{-1}$) (Table 3).

As regards the proposed reaction mechanism, regardless of the R group or the position that it occupies, the NH_2 group will always attack before the OH group in the case of *o*-aminophenols, while in the case of aromatic *o*-diamines, the amino group with the lowest chemical shift will attack first. In these mechanisms (Schemes 1 and 2), Steps 7 and 8 are the slowest since they involve a double migration of a proton.

Electrodonating groups such as methyl favour to the *para* position, and, as a consequence, the oxygen of the hydroxyl group in this position is more nucleophilic, while in electrowithdrawing groups (e.g. the carboxyl group), the *para* position is not favoured and so the oxygen of the hydroxyl group is less nucleophilic. Lastly, deprotonation of the aromatic *o*-diamines is much more difficult, which greatly slows down the oxidation process (Table 2).

We conclude therefore that deprotonation of the substrates in the action mechanism of tyrosinase is necessary, as we proposed previously [25,34,35], and that although the oxidation/reduction potentials are practically the same for both aromatic monoamines and phenols, the high *pK* of the amines slows down the reaction—data that agree with the results obtained for monophenols and *o*-diphenols [17,22,33].

In conclusion, we have demonstrated that mushroom TYR oxidises aromatic monoamines and *o*-diamines and *o*-aminophenols. For this oxidation process, we propose structural mechanisms that agree with the obtained experimental results and which show a certain parallelism to the mechanisms proposed for monophenolase and diphenolase activities of TYR [1,36,37]. In addition, we have kinetically characterised a wide number of substrates.

Acknowledgements

This paper was partially supported by grants from: Ministerio de Educación y Ciencia (Madrid, Spain) project BIO2009-12956, Fundación Séneca (CARM, Murcia, Spain) projects 08856/PI/08 and 08595/PI/08, andConsejería de Educación (CARM, Murcia, Spain) BIO-BMC 06/01-0004. JLMM and FGM hold two fellowships from Fundación Caja Murcia (Murcia, Spain).

Appendix A. Supplementary data

Supplementary data to this article can be found online at doi:10.1016/j.bbapap.2011.07.015.

References

[1] L. Fenoll, M.J. Peñalver, J.N. Rodriguez-Lopez, P.A. Garcia-Ruiz, F. Garcia-Canovas, J. Tudela, Deuterium isotope effect on the oxidation of monophenols and *o*-diphenols by tyrosinase, Biochem. J. 380 (2004) 643–650.
[2] A. Sanchez-Ferrer, J.N. Rodriguez-Lopez, F. Garcia-Canovas, F. Garcia-Carmona, Tyrosinase: a comprehensive review of its mechanism, Biochim. Biophys. Acta 1247 (1995) 1–11.
[3] E.I. Solomon, U.M. Sundaram, T.E. Machonkin, Multicopper oxidases and oxygenases, Chem. Rev. 96 (1996) 2563–2606.
[4] J.R. Jolley Jr., L.H. Evans, N. Makino, H.S. Mason, Oxytyrosinase, J. Biol. Chem. 249 (1974) 335–345.
[5] H. Decker, R. Dillinger, F. Tuczek, How does tyrosinase work? Recent insights from model chemistry and structural biology, Angew. Chem. Int. Ed. 39 (2000) 1591–1595.
[6] T. Klabunde, C. Eicken, J.C. Sacchettini, B. Krebs, Crystal structure of a plant catechol oxidase containing a dicopper center, Nat. Struct. Biol. 5 (1998) 1084–1090.
[7] Y. Matoba, T. Kumagai, A. Yamamoto, H. Yoshitsu, M. Sugiyama, Crystallographic evidence that the dinuclear copper center of tyrosinase is flexible during catalysis, J. Biol. Chem. 281 (2006) 8981–8990.
[8] M. Sendovski, M. Kanteev, V. Shuster Ben-Yosef, N. Adir, A. Fishman, Crystallization and preliminary X-ray crystallographic analysis of a bacterial tyrosinase from *Bacillus megaterium*, Acta Crystallogr. Sect. F Struct. Biol. Cryst. Commun. 66 (2010) 1101–1103.
[9] M. Sendovski, M. Kanteev, V. Shuster Ben-Yosef, N. Adir, A. Fishman, First structures of an active bacterial tyrosinase reveal copper plasticity, J. Mol. Biol. 405 (2011) 227–237.
[10] O. Toussaint, K. Lerch, Catalytic oxidation of 2-aminophenols and ortho hydroxylation of aromatic amines by tyrosinase, Biochemistry 26 (1987) 8567–8571.
[11] A. Rescigno, E. Sanjust, A.C. Rinaldi, F. Sollai, N. Curreli, A. Rinaldi, Effect of 3-hydroxyanthranilic acid on mushroom tyrosinase activity, Biochim. Biophys. Acta 1384 (1998) 268–276.
[12] E. Sanjust, G. Cecchini, F. Sollai, N. Curreli, A. Rescigno, 3-Hydroxykynureine as a substrate/activator for mushroom tyrosinase, Arch. Biochem. Biophys. 412 (2003) 272–278.
[13] F. Maddaluno, K.F. Faull, Inhibition of mushroom tyrosinase by 3-amino-L-tyrosine: molecular probing of the active site of the enzyme, Experientia 44 (1988) 885–887.
[14] B. Gasowska, P. Kafarski, H. Wojtasek, Interaction of mushroom tyrosinase with aromatic amines, *o*-diamines and *o*-aminophenols, Biochim. Biophys. Acta 1673 (2004) 170–177.
[15] F. Garcia-Molina, J.L. Muñoz, R. Varon, J.N. Rodriguez-Lopez, F. Garcia-Canovas, J. Tudela, A review on spectrophotometric methods for measuring the monophenolase and diphenolase activities of tyrosinase, J. Agric. Food Chem. 55 (2007) 9739–9749.
[16] J.N. Rodriguez-Lopez, J.R. Ros-Martinez, R. Varon, F. Garcia-Canovas, Calibration of a Clark-type oxygen electrode by tyrosinase-catalyzed oxidation of a 4-*tert*-butylcatechol, Anal. Biochem. 202 (1992) 356–360.
[17] J.N. Rodriguez-Lopez, L.G. Fenoll, P.A. Garcia-Ruiz, R. Varon, J. Tudela, R.N. Thorneley, F. Garcia-Canovas, Stopped-flow and steady-state study of the diphenolase activity of mushroom tyrosinase, Biochemistry 39 (2000) 10497–10506.

Scheme 3. Structural mechanism to explain the oxidation of aromatic *o*-diamines by TYR. E_m, met-tyrosinase; $(E_mS)_0$, met-tyrosinase/aromatic *o*-diamine complex; $(E_m\text{-}S)_1$, met-tyrosinase/aromatic *o*-diamine complex axially bound to a Cu atom with the base forming a hydrogen bridge; $(E_m\text{-}S)_2$, met-tyrosinase/aromatic *o*-diamine complex axially bound to a Cu atoms with protonated base; $(E_m\text{-}S)_3$, met-tyrosinase/aromatic *o*-diamine complex axially bound to the two Cu atoms; E_d, deoxy-tyrosinase; E_{ox}, oxy-tyrosinase; $(E_{ox}S)_0$, oxy-tyrosinase/aromatic *o*-diamine complex; $(E_{ox}\text{-}S)_1$, oxy-tyrosinase/aromatic *o*-diamine complex axially bound to a Cu atom; $(E_{ox}\text{-}S)_2$, oxy-tyrosinase/aromatic *o*-diamine complex axially bound to the two Cu atoms and with protonated base; $(E_{ox}\text{-}S)_3$, oxy-tyrosinase/aromatic o-diamine complex axially bound to the two Cu atoms with the proton transferred to the peroxide.

[18] M.M. Bradford, A rapid and sensitive method for the quantification of microgram quantities of proteins utilising the principle of protein–dye binding, Anal. Biochem. 72 (1976) 248–254.
[19] L.G. Fenoll, J.N. Rodriguez-Lopez, F. Garcia-Molina, F. Garcia-Canovas, J. Tudela, Michaelis constants of mushroom tyrosinase with respect to oxygen in the presence of monophenols and diphenols, Int. J. Biochem. Cell Biol. 34 (2002) 332–336.
[20] J.R. Ros, J.N. Rodriguez-Lopez, F. Garcia-Canovas, Tyrosinase: kinetics analysis of the transient phase and the steady state, Biochim. Biophys. Acta 1204 (1994) 33–42.
[21] Jandel Scientific., Sigma Plot 9.0 for Windows™, Jandel Scientific: Core Madera, 2006.
[22] J.L. Muñoz-Muñoz, F. Garcia-Molina, R. Varon, J. Tudela, F. Garcia-Canovas, J.N. Rodriguez-Lopez, New features of the steady-state rate related with the initial concentration of substrate in the diphenolase and monophenolase activities of tyrosinase, J. Math. Chem. 48 (2010) 347–362.
[23] K.D. Karlin, D.-H. Lee, H.V. Obias, K.J. Humphreys, Copper–dioxygen complexes: functional models of proteins, Pure Appl. Chem. 70 (1998) 855–862.
[24] L. Casella, E. Monzani, M. Gulloti, D. Cavagino, G. Cerina, L. Santagostini, R. Ugo, Functional modelling of tyrosinase. Mechanism of phenol ortho hydroxylation by dinuclear copper complexes, Inorg. Chem. 35 (1996) 7516–7625.
[25] F. García-Molina, J.L. Muñoz-Muñoz, M. Garcia-Molina, P.A. Garcia-Ruiz, J. Tudela, F. Garcia-Canovas, J.N. Rodriguez-Lopez, Melanogenesis inhibition due to NADH, Biosci. Biotechnol. Biochem. 74 (2010) 1777–1787.
[26] J.L. Muñoz-Muñoz, F. García-Molina, P.A. Garcia-Ruiz, R. Varon, J. Tudela, F. Garcia-Canovas, J.N. Rodriguez-Lopez, Stereospecific inactivation of tyrosinase by L- and D-ascorbic acid, Biochim. Biophys. Acta 1794 (2009) 244–253.
[27] F. García-Molina, J.L. Muñoz-Muñoz, J.R. Acosta, P.A. Garcia-Ruiz, J. Tudela, F. Garcia-Canovas, J.N. Rodriguez-Lopez, Melanogenesis inhibition by tetrahydropterines, Biochim. Biophys. Acta 1794 (2009) 1766–1774.
[28] F. García-Molina, J.L. Muñoz-Muñoz, F. Martinez-Ortiz, P.A. Garcia-Ruiz, J. Tudela, F. Garcia-Canovas, J.N. Rodriguez-Lopez, Tetrahydrofolic acid is a potent suicide substrate of mushroom tyrosinase, J. Agric. Food Chem. 59 (2011) 1383–1391.
[29] J.C. Espin, J. Tudela, F. Garcia-Canovas, 4-Hydroxyanisole: the most suitable monophenolic substrate for determining spectrophotometrically the monophenolase activity of polyphenol oxidase from fruits and vegetables, Anal. Biochem. 259 (1998) 118–126.
[30] J.L. Munoz, F. Garcia-Molina, R. Varon, J.N. Rodriguez-Lopez, F. Garcia-Canovas, J. Tudela, Calculating molar absorptivities for quinones: application to the measurement of tyrosinase activity, Anal. Biochem. 351 (2006) 128–138.
[31] L.G. Fenoll, J.N. Rodriguez-Lopez, R. Varon, P.A. Garcia-Ruiz, F. Garcia-Canovas, J. Tudela, Action mechanism of tyrosinase on meta- and para-hydroxylated monophenols, Biol. Chem. 381 (2000) 313–320.
[32] F.G. Molina, J.L. Munoz, R. Varon, J.N. Lopez, F.G. Canovas, J. Tudela, An approximate analytical solution to the lag period of monophenolase activity of tyrosinase, Int. J. Biochem. Cell Biol. 39 (2007) 238–252.
[33] D.E. Wilcox, A.G. Porras, Y.T. Hwang, K. Lerch, M.E. Winkler, E.I. Solomon, Substrate analogue binding to the coupled binuclear copper active site in tyrosinase, J. Am. Chem. Soc. 107 (1985) 4015–4027.
[34] J.L. Muñoz-Muñoz, F. Garcia-Molina, P.A. Garcia-Ruiz, M. Molina-Alarcon, J. Tudela, F. Garcia-Canovas, J.N. Rodriguez-Lopez, Phenolic substrates and suicide inactivation of tyrosinase: kinetics and mechanism, Biochem. J. 416 (2008) 413–440.
[35] J.L. Munoz-Munoz, F. Garcia-Molina, R. Varon, P.A. Garcia-Ruiz, J. Tudela, F. Garcia-Canovas, J.N. Rodriguez-Lopez, Suicide inactivation of the diphenolase and monophenolase activities of tyrosinase, IUBMB Life 62 (2010) 539–547.
[36] L. Fenoll, J.N. Rodriguez-Lopez, F. Garcia-Sevilla, P.A. Garcia-Ruiz, R. Varon, F. Garcia-Canovas, J. Tudela, Analysis and interpretation of the action mechanism of mushroom tyrosinase on monophenols and diphenols generating highly unstable *o*-quinones, Biochim. Biophys. Acta 1548 (2001) 1–22.
[37] M.J. Penalver, J.N. Rodriguez-Lopez, P.A. Garcia-Ruiz, F. Garcia-Canovas, J. Tudela, Solvent deuterium isotope effect on the oxidation of *o*-diphenols by tyrosinase, Biochim. Biophys. Acta 1650 (2003) 128–135.